ANALYSIS AND EXPERIMENTAL REALIZATION OF A HYBRID ELECTRO-VISCOELASTIC VIBRATION NEUTRALIZER

Rodrigo Féder Paraná, rfparana@gmail.com
Universidade Federal Tecnológica do Paraná - UTFPR Av. Sete de Setembro, 3165 Curitiba - PR

Carlos Alberto Bavastri, bavastri@ufpr.br
Universidade Federal do Paraná - UFPR Av. Cel. Francisco H. dos Santos, s/n Curitiba - PR

Abstract. *Dynamic Vibration Neutralizers have been used for almost a century to reduce vibration and acoustical noise in many mechanical structures. Nowadays, viscoelastic neutralizers are used due to their accurate and simple modeling by fractional calculus and generalized quantities as well as their easy manufacturing and design advantages such the wideband application and significant energy dissipation. However, the viscoelastic material characteristics change as temperature varies, causing detuning and low performance. In the present work, a hybrid electro-viscoelastic dynamic vibration neutralizer is presented. The electrodynamical component of this neutralizer is made of a permanent magnet, a moving coil and a connected electric circuit. Its goal is to compensate temperature-detuning loss. Numerical simulations quantify the detuning phenomenon. Optimum performance for the hybrid neutralizer is achieved with nonlinear optimization tchniques and its behavior is analyzed in different situations. Numerical simulations include the device performance with temperature variation, different viscoelastic materials, primary system mass and natural frequency variation. A prototype device was built and measurements were compared with simulations. Results are discussed and indicate the device application field.*

Keywords*: Vibration control, Electro-viscoelastic neutralizer, Viscoelastic material, Nonlinear optimization techniques*

1. INTRODUCTION

Vibration neutralizers are simple mechanical devices for attaching to another mechanical system or structure, the primary system, to control or reduce vibration and sound radiation from machines or structural surfaces. Vibration neutralizers were first used to reduce rolling motions of ships (Frahm, 1909). Since then, many publications on the subject have demonstrated their efficiency in reducing vibrations and sound radiation in many kinds of structures and machines (Den Hartog, 1956).

With the use of viscoelastic materials, which can be manufactured to meet design specifications, vibration neutralizers had become easy to make and apply to almost any complex structure (Bavastri, 1997; Snowdon, 1968).

Espíndola and Silva (1992) presented a general theory for optimum design of neutralizer systems, when applied to generic structures. This approach has been successfully applied to many types of viscoelastic neutralizers (Freitas and Espíndola, 1993; Bavastri and Espíndola, 1995; Espíndola and Bavastri, 1997). The theory was based on the concept of equivalent generalized quantities for the neutralizers. With this concept, it is possible to write down the composite system (primary plus absorbers) motion equations in terms of the generalized coordinates (degrees of freedom), previously chosen to describe the primary system alone, despite the fact that the composite system has additional degrees of freedom (Espíndola and Bavastri, 1999). A nonlinear optimization technique can be used to design the neutralizer system to be optimum, in a certain sense, over a specific frequency band.

The concept of fractional derivative is applied to the construction of a parametric model for the viscoelastic material (Espíndola *et al*., 2004). Viscoelastic materials are both frequency and temperature dependent. Thus, a disadvantage for the use of such material is that vibration neutralizers designed to optimally work in a specific frequency range, when exposed to temperature variations, can be detuned.

Electromechanical vibration neutralizers use the interaction between a magnetic field and the displacement of a coil to generate an electromotive force in a resonant RLC electrical circuit. The resulting circuit current generates a magnetic force that can reduce the primary system vibration (Bavastri, 2001; Abu-Akeel, 1967; Nagem *et al*., 1995). Such neutralizers can be set as passive or active control devices by varying RLC parameters. However, there are practical difficulties because they must be installed with an auxiliary structure to support the magnetic field generator.

To combine benefits of both viscoelastic and electromechanical vibration neutralizers, a new model of hybrid viscoelastic-electromechanical vibration neutralizer (HEVDN) was presented (Hudenski *et al*., 2007; Paraná, 2008). This neutralizer is made of two resonant systems: one mechanical and one electromechanical. The former is made of a tuning mass and a viscoelastic material. The viscoelastic material holds together the tuning mass to the frame that is attached to the primary system. The frame also holds the magnet, and its magnetic field involves the tuning mass. Around the tuning mass there is a coil that is linked to a resonant RLC electric circuit. Thus, when there is relative displacement between the coil around the tuning mass and the magnetic field, an electromotive force is generated in the electric circuit. This hybrid neutralizer can achieve optimal vibration reduction and act as an active vibration control device by changing the electrical circuit parameters or by applying voltage to the coil terminals. This characteristic can be used to retune the neutralizer if it is exposed to temperature variation. Additionally, the hybrid configuration does not need to be installed with an auxiliary structure. Figure 1 shows the hybrid electro-viscoelastic vibration neutralizer configuration.

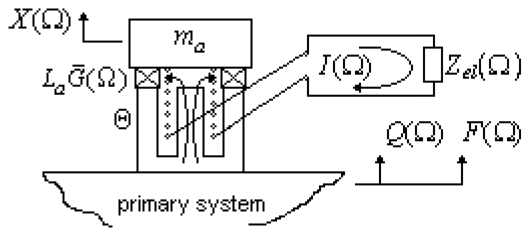

Figure 1. Electro-viscoelastic vibration neutralizer configuration

2. THE HYBRID MODEL

Conceptually, the vibration neutralizer's goal is to offer to the vibrating system high mechanical impedance in a certain frequency range, in which the system has low mechanical impedance. It is shown that, in this range, there are one or more natural frequencies to be controlled, and, for this reason, system mechanical impedance is low. The mechanical impedance $Z_b(\Omega)$ offered by the hybrid neutralizer to the primary system is given by Eq. (1) (Paraná, 2008), in which Ω is the circular frequency, $F(\Omega)$ is the excitation force, $Q(\Omega)$ is the primary system displacement, m_a is the tuning mass, Θ is the magnetic coupling strength factor, $Z_{el}(\Omega)$ is the electrical impedance, L_a is the shape factor and $i=\sqrt{-1}$.

$$Z_b(\Omega)=\frac{F(\Omega)}{i\Omega Q(\Omega)}=\frac{-i\Omega^3 m_a\Theta^2-\Omega^2 m_a L_a\overline{G}(\Omega)Z_{el}(\Omega)}{-\Omega^2\Theta^2+i\Omega Z_{el}(\Omega)\left(-\Omega^2 m_a+L_a\overline{G}(\Omega)\right)}. \tag{1}$$

In order to proceed with numerical simulations, it is necessary to express Eq. (1) nondimensionally with respect to L_a.

The fractional derivative model describes the linear behavior of thermorheologically simple viscoelastic materials (Bagley and Torvik, 1986; Pritz, 1996). These materials have a complex shear modulus, where the real part accounts for the storage of energy and the imaginary part for the dissipation of energy. In the frequency domain, the complex shear modulus is given by

$$\overline{G}(\Omega,T)=\frac{G_L+G_H\phi_0(i\Omega_R)^\beta}{1+\phi_0(i\Omega_R)^\beta}. \tag{2}$$

The reduced frequency is given by $\Omega_R=\alpha_T(T)\,\Omega$ and the shift factor α_T is

$$\log_{10}\alpha_T(T)=\frac{-\theta_1(T-T_0)}{\theta_2+(T-T_0)}. \tag{3}$$

In Eq. (2) and Eq. (3), T is the absolute temperature, T_0 is the reference temperature, G_L, G_H, ϕ_0, β, θ_1 and θ_2 are experimentally determined parameters.

The equivalent quantities $m_{eq}(\Omega)$ and $c_{eq}(\Omega)$, generalized equivalent mass and damping, respectively, were obtained by Paraná (2008) with the relation

$$Z_b(\Omega)=c_{eq}(\Omega)+i\Omega m_{eq}(\Omega). \tag{4}$$

Therefore, an equivalent model to the hybrid neutralizer is obtained, as shown in Fig. 2. The frequency response of the whole system is expressed in Eq. (5), in which, m, c and k are the primary system mass, damping factor and stiffness.

$$H(\Omega) = \frac{1}{-\Omega^2\left(m + m_{eq}(\Omega)\right) + i\Omega\left(c + c_{eq}(\Omega)\right) + k}. \tag{5}$$

The optimization problem consists of minimizing the objective function

$$f(\mathbf{x}) = \max_{\Omega_1 < \Omega < \Omega_2} \left|H(\Omega, \mathbf{x})\right| \tag{6}$$

subjected to the inequality constraint

$$\mathbf{x}_L < \mathbf{x} < \mathbf{x}_U \tag{7}$$

in which Ω_1 and Ω_2 are the lower and upper limits of the frequency range of concern, respectively, $\mathbf{x}$ is the design vector, $\mathbf{x}_L$ and $\mathbf{x}_U$ are lower and upper constraint vectors. To perform the optimization, $\mathbf{x} = \left[\Omega_a, R, L, C\right]$ and the viscoelastic neutralizer natural frequency $\Omega_a = \sqrt{\frac{L_a G(\Omega_a)}{m_a}}$.

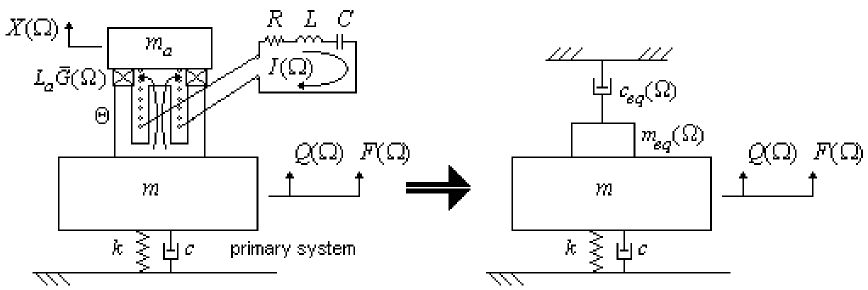

Figure 2. Equivalent quantities for the electro-viscoelastic vibration neutralizer

3. NUMERICAL SIMULATIONS

3.1. Analyzed configurations and preliminar considerations

The aim of the numerical simulations is to verify the hybrid vibration neutralizer performance with respect to parametrical variations. The most important parameter to consider is temperature, that changes the viscoelastic material properties, causing detuning. Thus, the function of the electrodynamical component is to compensate vibration reduction losses.

A series of configurations for the primary system have been simulated, including combinations of primary system mass m_{sp} (5, 50 and 500 kg) and primary system natural frequency Ω_{sp} (50, 300 and 600 Hz). Three distinct temperatures have been simulated: the design temperature T_i (25 °C) and two detuning temperatures T_f (- 10 °C and 60 °C).

An elementary primary system with only one degree-of-freedom is used in all simulations to better understand the performance of the attached vibration neutralizer. The damping factor adopted is null.

The magnetic assemble and moving coil of a commercial loudspeaker can be used to build the electrodynamical component of the hybrid vibration neutralizer. Table 1 shows parameter values used in simulations. The moving coil resistance R_e and inductance L_e were estimated by Paraná (2008). The influence of temperature variation upon the resistance is considered negligible. The magnetic assemble mass m_c varies considerably. Therefore, for each primary system mass configuration, a reasonable related loudspeaker model was used. In all cases, mass relation $\mu = m/m_a = 0{,}05$.

The analysis procedure is as follows. Firstly, considering the electrical circuit off, the mathematical model of the hybrid vibration neutralizer is equal to the pure viscoelastic one. With the electrical circuit turned off ($\Theta = 0$), viscoelastic optimization is done, outputting the optimum viscoelastic natural frequency, referred to design temperature T_i, that minimizes the primary system vibration. Secondly, the electrical circuit resistance R, inductance L and capacitance C are optimized, considering temperature variation detuning or not. The electrical variable optimization at design temperature is done to verify if the electrodynamical component improves the viscoelastic performance. To measure detuning effects, the detuning gain G_D is defined comparing frequency responses maximum values before and after temperature variation; the retuning gain G_R is calculated comparing frequency responses maximum values after temperature variation and after electrical circuit optimization to determine improvements made by the electrodynamical component. The total gain $G_T = G_R + G_D$.

Table 1. Loudspeaker: models and parameter values.

Manufacturer/ model	m_c (kg)	Θ (Tm)	R_e (Ω)	L_e (mH)
SELENIUM/ Driver Titanium D2500Ti-Nd	0,66	4,7	7,0	1,0
SELENIUM/ Woofer 15PW5	6,22	17,0	9,0	2,0
SELENIUM/ Subwoofer 18SW2P	8,60	25,4	13,0	5,0

3.2. Results

Table 2 lists some of the obtained results. Light gray indicated simulations showing results in which $G_R \geq 2$ dB and dark gray indicated simulations showing results in which $G_T \geq 0{,}5$ dB. The index "*" express obtained optimum values. The electric circuit natural frequency is $\Omega_{el} = \sqrt{1/LC}$. Best results are shown in Fig. 3. Simulation 1 shows a significant retuning effect after temperature increases to 60 ^{o}C and the electric circuit is turned on and optimized. Simulation 2 shows that, even with no temperature variation, a certain gain is obtained when the electrodynamical component is active. Simulations 3 and 4 show high temperature detuning when a viscoelastic material other than neoprene is used. In these cases, although retuning gains are high, overall performance is influenced by the high variation of the characteristics of the viscoelastic materials.

None of the simulations with T_f = -10 ^{o}C resulted in significant performance gains. Actually, in these cases, almost all gains were null. At this temperature, the shear modulus of the tested viscoelastic materials rises considerably. With such high shear modulus, relative displacement between the tuning mass and primary system is very low and the electric circuit action does not occur.

The detuning temperature T_f = 60 ^{o}C was used in simulations that indicated a significant action of the neutralizer, with $G_R \geq 2$ dB. These best results occurred with the three viscoelastic materials, low natural frequency of the primary system (50 Hz) and low and medium mass values (5 and 50 kg). In these cases, the optimum circuit natural frequency is very close to the primary system natural frequency and the optimum resistance is always minimum. Thus, in these cases, the magnetic force F_M applied by the electrodynamical component, expressed by Eq. (8), is maximum, so to enhance the mechanical impedance provided by the vibration neutralizer.

$$F_M(\Omega) = \frac{\Theta^2 i\Omega\left(Q(\Omega) - X(\Omega)\right)}{Z_{el}(\Omega)}. \tag{8}$$

The increase of the primary system mass to 50 kg results in very similar gains. This occurs because the magnetic force increases proportionally with the loudspeaker model used. The same does not occur if the primary system mass is 500 kg, which results in insignificant gains.

It can be observed that, although gains highlighted in Table 2 are significant, in the cases in which pure butylic rubber and EAR Isodamp C-1002 were used, detuning with temperature rise is very intense and the total gain is almost not perceptible in graphics. At high temperatures, viscoelastic material shear modulus and loss factor are lower. For these materials, variation is high. For neoprene, loss factor reduction is more significant. Thus, in this case, it is clear that the electrodynamical component action is to add a damping force to the system, in order to compensate damping loss due to temperature increase.

Increasing primary system natural frequency results in total gain decreases. This situation may be explained analyzing Eq. (8). Although a higher frequency could make the magnetic force increase, the relative displacement reduction is more significant, making the magnetic force and, consequently, the total gain, decrease.

Table 3 shows simulations with a two times higher magnetic coupling strength factor, showing a general improvement in results. Best results occur at T_f = 60 ^{o}C, no matter the viscoelastic material used. There are significant total gains for any simulated primary system mass value and for higher frequencies (300 Hz). Simulations 1b and 28b show positive total gain even with temperature detuning, i.e., a better performance than the pure viscoelastic control, even with temperature rise.

A set of simulations in which R, L, C and Ω_a are optimized at the same time was conducted with no significantly better results.

As the magnetic force increases with electric impedance reduction, a short-circuited model of the moving coil was simulated. Results show similar gains with the optimum values obtained for the electric circuit. Figure 4 compares the simulations.

Table 2. Simulation results.

simul.	m (kg)	Ω_{sp}(Hz)	Viscoelastic Material	Ω_a* (Hz)	T_f (ºC)	R* (Ω)	L* (mH)	C* (μF)	Ω_{el}* (Hz)	G_D (dB)	G_R (dB)	G_T (dB)
1	5	50	neoprene	48,2	60	7,0	132,8	68,6	52,7	-14,6	7,0	-7,7
2	5	50	neoprene	48,2	25	7,0	88,1	130,5	46,9	0,0	1,6	1,6
3	5	50	neoprene	48,2	-10	7,0	160,6	61,0	50,9	-22,5	0,1	-22,4
4	5	50	pure butylic	46,6	60	7,0	109,1	92,5	50,1	-22,5	4,5	-18,0
5	5	50	pure butylic	46,6	25	10000,0	1,0	6066,0	64,6	0,0	0,0	0,0
6	5	50	pure butylic	46,6	-10	7,0	80,8	121,7	50,7	-30,1	0,1	-30,0
7	5	50	EAR Isodamp	40,5	60	7,0	131,2	75,9	50,4	-32,7	9,6	-23,1
8	5	50	EAR Isodamp	40,5	25	10000,0	1,0	32542,0	27,9	0,0	0,0	0,0
9	5	50	EAR Isodamp	40,5	-10	7,0	1,0	200,3	355,6	-36,9	0,0	-36,9
10	5	300	neoprene	286,2	60	7,0	4,4	67,1	293,8	-16,2	0,9	-15,3
11	5	300	neoprene	286,2	25	7,0	19,9	14,7	294,0	0,0	0,1	0,1
12	5	300	neoprene	286,2	-10	7,0	1,0	105,8	489,2	-29,8	0,0	-29,8
13	5	300	pure butylic	273,5	60	7,0	1,0	666,6	194,9	-22,3	0,8	-21,6
14	5	300	pure butylic	273,5	25	7,0	26,7	28,2	183,3	0,0	0,0	0,0
15	5	300	pure butylic	273,5	-10	7,0	12,2	19,7	324,7	-29,8	0,0	-29,8
16	5	300	EAR Isodamp	227,9	60	7,0	7,2	50,8	264,0	-30,0	1,5	-28,6
17	5	300	EAR Isodamp	227,9	25	7,0	14,0	58,3	176,4	0,0	0,0	0,0
18	5	300	EAR Isodamp	227,9	-10	7,0	2,1	208,8	241,1	-35,3	0,0	-35,3
19	5	600	neoprene	569,0	60	7,0	1,0	54,5	682,0	-14,6	0,2	-14,4
20	5	600	neoprene	569,0	25	7,0	16,0	4,3	606,7	0,0	0,0	0,0
21	5	600	neoprene	569,0	-10	7,0	741,1	0,1	584,6	-31,6	0,0	-31,6
22	5	600	pure butylic	543,4	60	7,0	13,0	5,3	604,8	-10,1	0,2	-9,9
23	5	600	pure butylic	543,4	25	7,0	8,8	79,8	189,9	0,0	0,0	0,0
24	5	600	pure butylic	543,4	-10	7,0	19,0	3,9	587,7	-29,7	0,0	-29,7
25	5	600	EAR Isodamp	450,2	60	7,0	1,6	200,4	281,1	-39,4	1,5	-37,8
26	5	600	EAR Isodamp	450,2	25	7,0	4,7	281,9	138,5	0,0	0,0	0,0
27	5	600	EAR Isodamp	450,2	-10	7,0	3,4	24,6	550,2	-37,4	0,0	-37,4
28	50	50	neoprene	48,2	60	9,0	48,9	201,3	50,7	-14,6	7,1	-7,6
29	50	50	neoprene	48,2	25	9,0	97,0	116,1	47,4	0,0	1,6	1,6
30	50	50	neoprene	48,2	-10	9,0	182,3	53,1	51,2	-22,5	0,1	-22,4
31	50	50	pure butylic	46,6	60	9,0	86,5	119,4	49,5	-22,5	4,6	-18,0
32	50	50	pure butylic	46,6	25	10000,0	2,0	9105,7	37,3	0,0	0,0	0,0
33	50	50	pure butylic	46,6	-10	9,0	78,7	121,7	51,4	-30,1	0,1	-30,0
34	50	50	EAR Isodamp	40,5	60	9,0	118,3	84,0	50,5	-32,7	9,7	-23,0

Table 3. Simulation results – two times higher magnetic coupling strength factor.

simul.	m (kg)	Ω_{sp}(Hz)	Viscoelastic Material	Ω_a* (Hz)	T_f (ºC)	R* (Ω)	L* (mH)	C* (μF)	Ω_{el}* (Hz)	G_D (dB)	G_R (dB)	G_T (dB)
1b	5	50	neoprene	48,2	60	7,0	54,6	194,0	48,9	-14,6	15,1	0,5
2b	5	50	neoprene	48,2	25	8,3	78,9	127,6	50,1	0,0	3,8	3,8
3b	5	50	neoprene	48,2	-10	7,0	161,4	60,5	50,9	-22,5	0,5	-22,1
4b	5	50	pure butylic	46,6	60	7,0	59,5	187,3	47,7	-22,5	11,3	-11,2
5b	5	50	pure butylic	46,6	25	10000,0	1,0	6066,0	64,6	0,0	0,0	0,0
6b	5	50	pure butylic	46,6	-10	7,0	80,6	121,6	50,9	-30,1	0,4	-29,7
7b	5	50	EAR Isodamp	40,5	60	7,0	133,0	77,4	49,6	-32,7	19,1	-13,5
8b	5	50	EAR Isodamp	40,5	25	10000,0	1,0	32542,0	27,9	0,0	0,0	0,0
9b	5	50	EAR Isodamp	40,5	-10	7,0	1,0	199,2	356,6	-36,9	0,0	-36,9
10b	5	300	neoprene	286,2	60	7,0	4,9	61,8	289,3	-16,2	3,2	-13,0
11b	5	300	neoprene	286,2	25	7,0	14,6	18,4	307,2	0,0	0,4	0,4
12b	5	300	neoprene	286,2	-10	7,0	1,0	105,1	490,9	-29,8	0,1	-29,7
13b	5	300	pure butylic	273,5	60	7,0	1,0	747,8	184,0	-22,3	2,7	-19,6
14b	5	300	pure butylic	273,5	25	7,0	26,7	29,2	180,3	0,0	0,0	0,0
15b	5	300	pure butylic	273,5	-10	7,0	2967,9	0,1	292,1	-29,8	0,1	-29,8
16b	5	300	EAR Isodamp	227,9	60	7,0	3,7	102,7	257,0	-30,0	4,9	-25,1
17b	5	300	EAR Isodamp	227,9	25	7,0	14,0	59,8	174,2	0,0	0,1	0,1
18b	5	300	EAR Isodamp	227,9	-10	7,0	2,0	208,9	243,4	-35,3	0,0	-35,3
19b	5	600	neoprene	569,0	60	7,0	1,0	53,4	689,0	-14,6	0,7	-13,8
20b	5	600	neoprene	569,0	25	7,0	10000,0	46,1	7,4	0,0	0,0	0,0
21b	5	600	neoprene	569,0	-10	7,0	741,1	0,1	584,6	-31,6	0,0	-31,6
22b	5	600	pure butylic	543,4	60	7,0	12,2	5,7	603,0	-10,1	0,7	-9,4
23b	5	600	pure butylic	543,4	25	7,0	8,9	79,8	188,9	0,0	0,0	0,0
24b	5	600	pure butylic	543,4	-10	7,0	18,8	3,9	587,8	-29,7	0,0	-29,6
25b	5	600	EAR Isodamp	450,2	60	7,0	4,5	16,3	584,5	-10,9	0,9	-10,0
26b	5	600	EAR Isodamp	450,2	25	7,0	4,7	282,7	138,0	0,0	0,0	0,0
27b	5	600	EAR Isodamp	450,2	-10	7,0	7,6	10,2	570,9	-37,4	0,0	-37,4
28b	50	50	neoprene	48,2	60	9,0	58,4	190,1	47,8	-14,6	15,2	0,6
29b	50	50	neoprene	48,2	25	10,8	76,4	127,6	51,0	0,0	3,8	3,8
30b	50	50	neoprene	48,2	-10	9,0	181,3	53,2	51,3	-22,5	0,5	-22,0
31b	50	50	pure butylic	46,6	60	9,0	90,4	120,9	48,1	-22,5	11,4	-11,1
32b	50	50	pure butylic	46,6	25	10000,0	2,0	48544,3	16,2	0,0	0,0	0,0
33b	50	50	pure butylic	46,6	-10	9,0	78,3	121,7	51,6	-30,1	0,4	-29,7
34b	50	50	EAR Isodamp	40,5	60	9,0	116,3	89,8	49,3	-32,7	19,3	-13,4

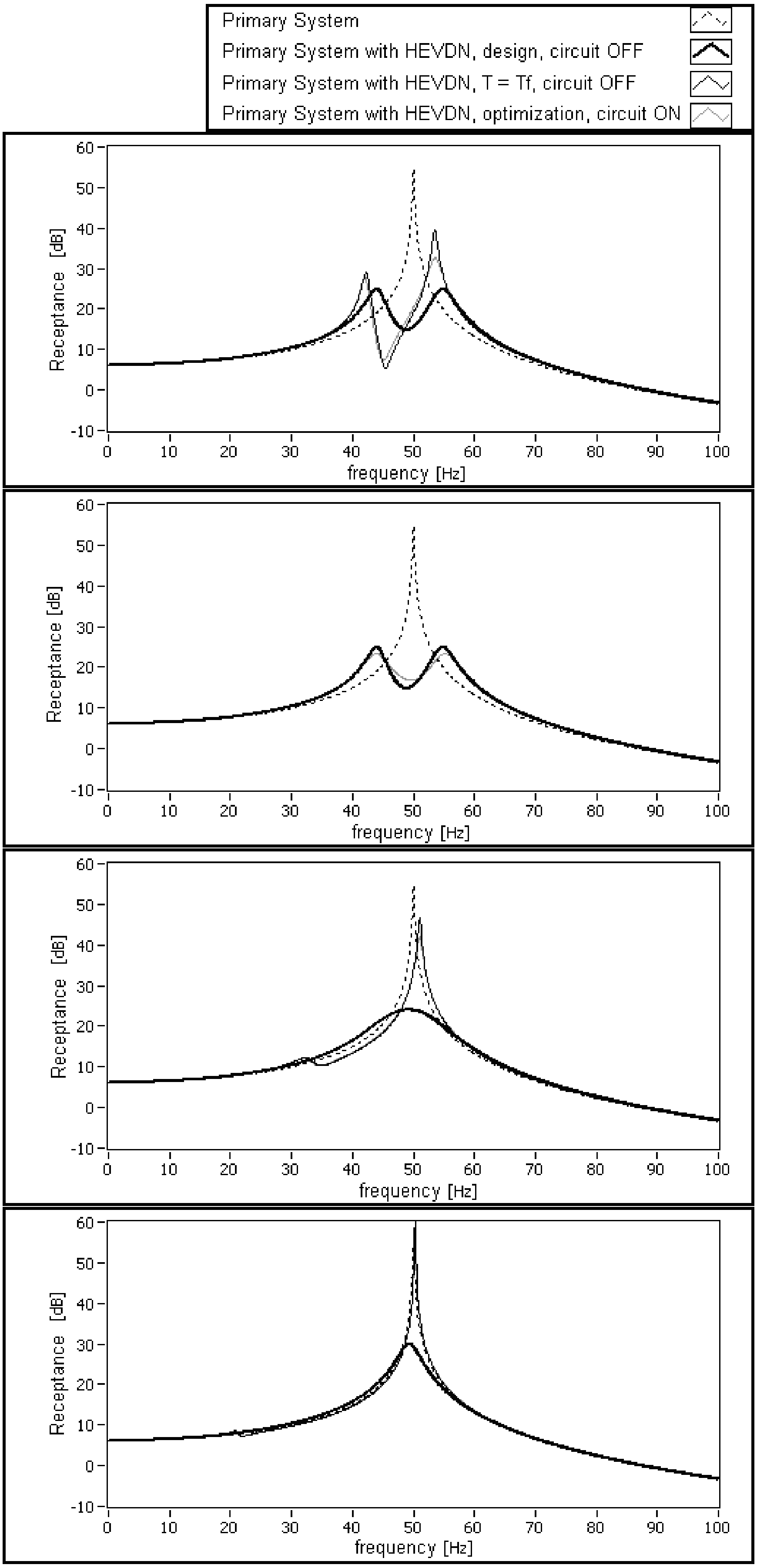

Figure 3. Simulations 1, 2, 4 and 7

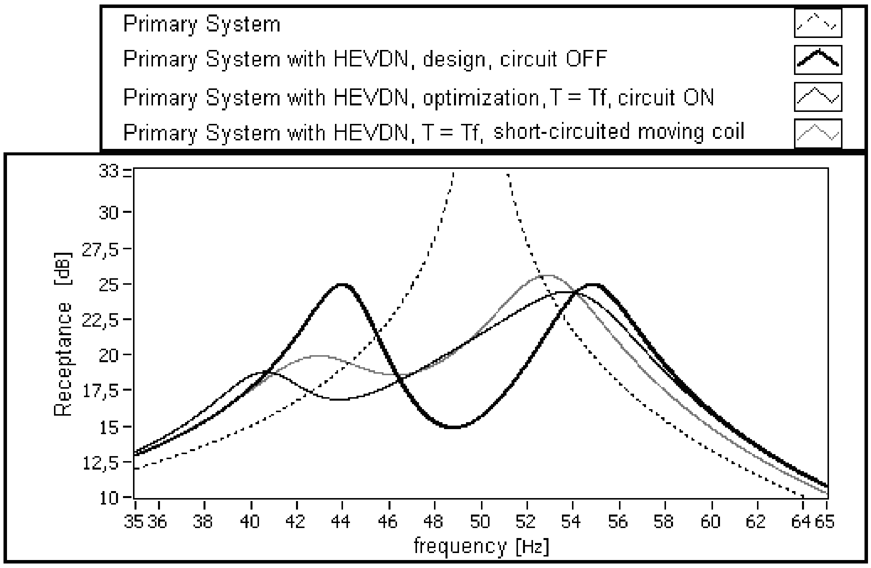

Figure 4. Comparison: simulation 1b versus short-circuited moving coil

4. EXPERIMENTAL REALIZATION

4.1. Design

A hybrid electro-viscoelastic dynamic neutralizer was designed considering data presented in Table 4. The viscoelastic material neoprene 48 Shore A was used. To build the electrodynamical component of the neutralizer, a commercial loudspeaker, SELENIUM Driver Titanium D2500Ti-Nd, was used.

Figure 5 shows the neutralizer pieces. The magnetic assemble and frame mass m_c is considered as part of the primary system mass. The frame is used to hold the iron-made tuning mass. The moving coil is attached to the tuning mass through an acrylic cylinder. The obtained shape factor L_a leads to thin rubber pieces.

Table 4. Design data.

Variable	Value	Variable	Value	Variable	Value	Variable	Value
m_a (kg)	0,2	Ω_a* (Hz)	43,4	Θ (Tm)	4,7	Number of parallel rubber pieces	3
Ω_{sp}(Hz)	45	L_a (m)	0,001174	R_e (Ω)	7,0		
T_i (^{o}C)	25	m_c (kg)	0,82	L_e (mH)	1,0		

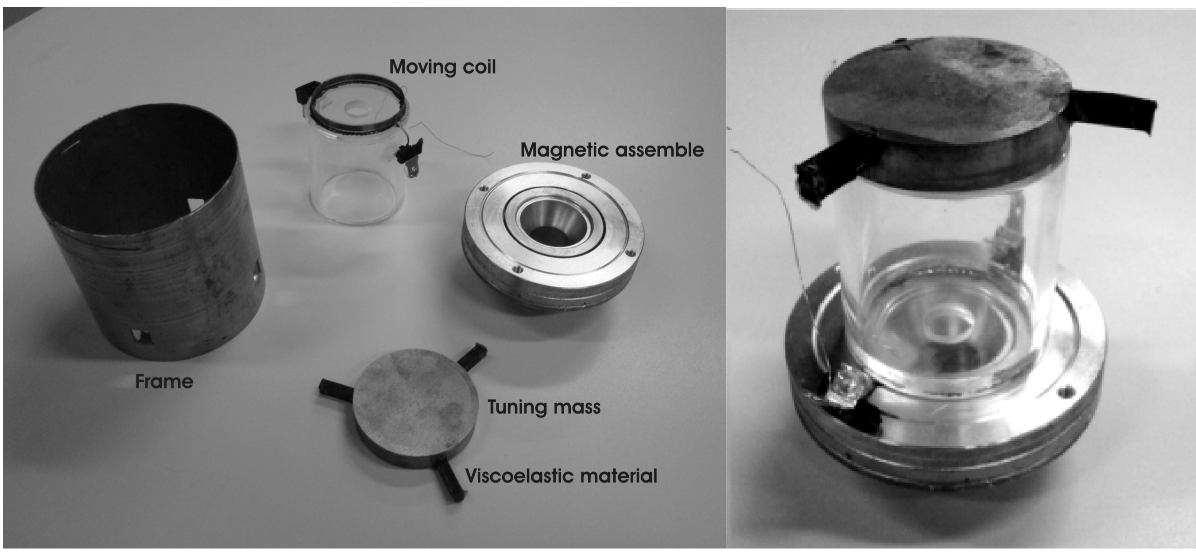

Figure 5. Neutralizer pieces and mounting process

4.2. Experiment

The frequency response function (inertance) of the hybrid neutralizer was measured at $T_f = 24\ ^oC$. An accelerometer PCB Piezotronics 352C68, an impact hammer PCB Piezotronics 086C04 and a data acquisition system LDS Photon+ / RT Pro Photon v 6.33 were used. All measurements are referred to m/(Ns^2). An exponential force spectral window with low damping was used. Figure 6 shows the measurement scheme, with the accelerometer mounted on the neutralizer running mass. Figure 7 shows the obtained response, with $\Omega_a(T_f) = 41{,}3$ Hz. The viscoelastic natural frequency obtained is close to the simulated one, $\Omega_a(T_f) = 43{,}6$ Hz.

The primary system is made of an aluminum block mounted on springs. Its natural frequency, considering the magnetic assemble mass, is $\Omega_{sp} = 46{,}2$ Hz. The frequency response of the composite system (primary system plus neutralizer) was measured at $T = 26\ ^oC$, with the electric circuit turned off, and at a detuning temperature $T_f = 48\ ^oC$, with the electric circuit turned on and off. The electric circuit is the short-circuited moving coil. Figure 6 shows the measurement scheme. The viscoelastic material was heated during one minute with an ordinary hair-dryer. Thermocouples measure room and neoprene temperatures. Figure 8 shows the obtained frequency responses. As expected, when temperature rises, detuning causes performance loss. The reduction G_D = -4,1 dB. When the moving coil is short-circuited, there is a significant improvement G_R = 2,7 dB. The total gain G_T = -1,4 dB. The gains are lower then those obtained by simulation for the same conditions. To equal experimental and simulation gains, the detuning temperature must be $T_f = 33\ ^oC$ and $R_e = 14\ \Omega$ or $\Theta = 3{,}3$ Tm. Figure 9 shows this simulation.

Figure 6. Neutralizer inertance measurement scheme (left) and composite system inertance measurement scheme (right)

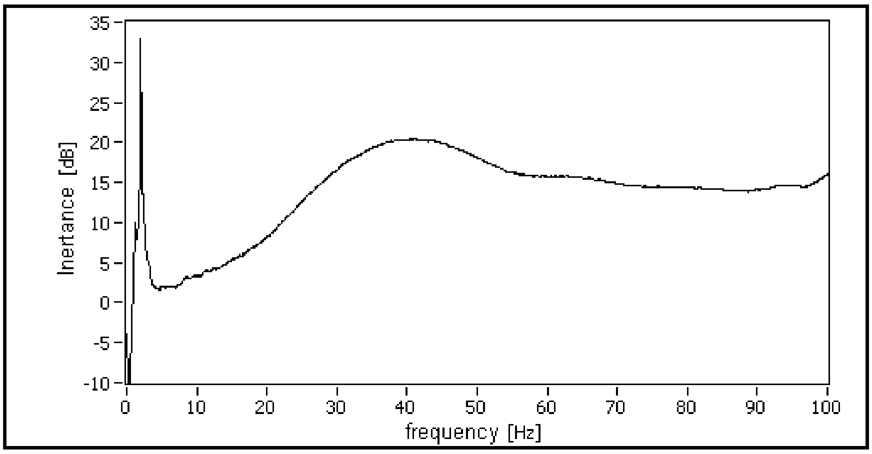

Figure 7. Neutralizer frequency response

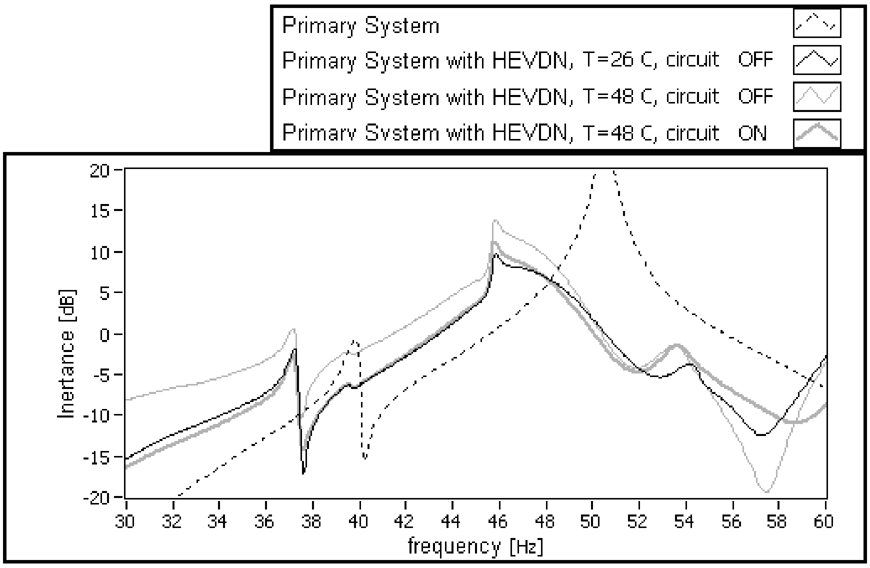

Figure 8. Composite system frequency responses

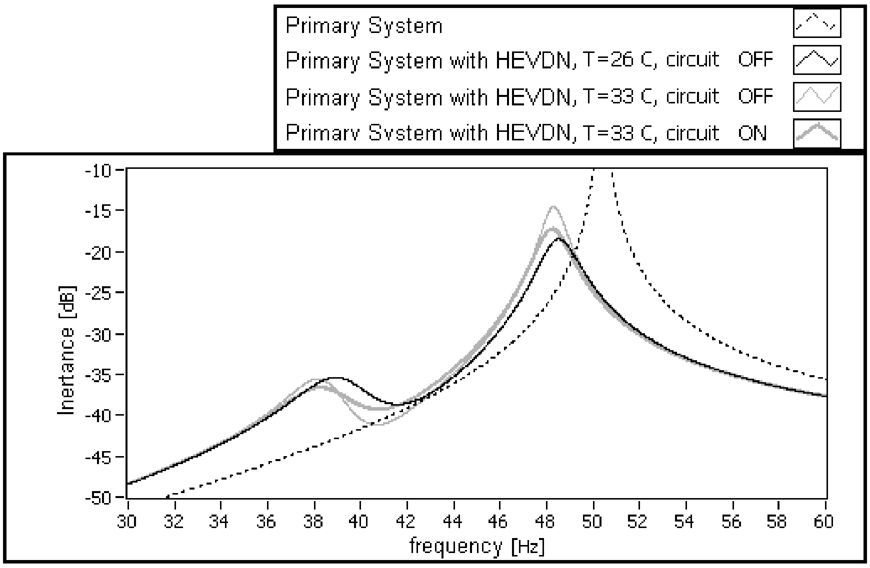

Figure 9. Comparative simulation

5. CONCLUSIONS

Through simulations, the optimum behavior of the hybrid dynamic vibration neutralizer was analyzed in different situations, including temperature variation, primary system mass and natural frequency variations, as well as the use of three different viscoelastic materials. This new proposed model benefits from both viscoelastic and electromechanical neutralizers and does not need auxiliary structures. Firstly, a viscoelastic optimization with the electric circuit turned off is made. Then, an intentional detune caused by temperature variation is simulated and a second optimization, now upon the electric circuit parameters, is made.

It was verified that the neutralizer performance is improved with a higher magnetic coupling strength factor and is more significant for temperatures higher than designed and low primary system natural frequencies. At low temperatures, the viscoelastic material shear modulus rises considerably constraining the moving coil relative displacement. In case of high primary system natural frequencies, the relative displacement amplitude of the moving coil decreases significantly, reducing magnetic force and the neutralizer performance. With a short-circuited moving coil, similar results were obtained. Good performances were obtained with the three viscoelastic materials simulated. However, neoprene has a lower shear modulus variation with temperature and higher damping loss. These characteristics make the hybrid neutralizer achieve better results by adding damping to the system.

A prototype device was built and measurements confirmed its action in compensating temperature-detuning loss. The experiment must be redone in a proper temperature chamber to achieve homogeneous temperature in the viscoelastic material in order to obtain a better coincidence between simulation and experimental results.

This study demonstrates that it is possible to design and build a hybrid electro-viscoelastic vibration neutralizer to compensate detuning losses in viscoelastic control caused by temperature variation.

6. ACKNOWLEDGEMENTS

This work was partially supported by the Brazilian government agency FINEP through project PROMOVE 4931-06.

7. REFERENCES

Abu-Akeel, A.K., 1967. "The Electrodynamic Vibration Absorber as a Passive or Active Device". *Journal of Engineering for Industry*. pp.741-753.

Bagley, R.L. and Torvik, P.J. 1986. "On the Fractional Calculus Model of Viscoelastic Behavior". *Journal of Reology* (30) 133-155.

Bavastri, C.A. and Espíndola, J.J., 1995. "Reduction of Vibrations in complex Structures with Viscoelastic neutralizers: a Generalized Approach", *Proceedings of ASME Design Engineering Technical Conferences*. pp.761-766.

Bavastri, C.A., 1997, "Reduções de Vibrações de Banda Larga em Estruturas Complexas por Neutralizadores Viscoelásticos". Doctorate Thesis, Universidade Federal de Santa Catarina, Brasil.

Bavastri, C.A., 2001, "Neutralizador Electromecânico de Vibraciones: Parâmetros Equivalentes Generalizados". *In: XII ENIEF, Congress on Numerical Methods and their Applications, Argentina.*

Den Hartog, J.P., 1956. "Mechanical Vibrations". New York: McGraw-Hill.

Espíndola, J.J. and Silva, H.P., 1992. "Modal Reduction of Vibrations by Dynamic Neutralizers", *Proceedings of the Tenth International Modal Analysis Conference, San Diego, USA*. pp. 1367-1373.

Espíndola, J.J. and Bavastri, C.A., 1997. "Reduction of Vibrations in complex Structures with Viscoelastic neutralizers: a Generalized Approach and a Physical Realization", *Proceedings of DETC´97 ASME Design Engineering Technical Conferences, Sacramento, USA*. pp.251-258.

Espíndola, J.J. and Bavastri, C.A., 1999. "Optimum Conceptual Design of Viscoelastic Dynamic Vibration Neutralizer for Low Frequency Complex Structures", *EURODiname 99*, pp.251-258.

Espíndola, J.J., Silva Neto, J.M. and Lopes, E.M.O., 2004. "A New Approach to Viscoelastic Material Properties Identification Based on the Fractional Derivative Model". *Proceedings of First IFAC Workshop on Fractional Differentiation and its Application (FDA' 04), Bordeaux, France*.

Frahm, H., 1909. "Device for Damping Vibration of Bodies", U.S. Patent n^{o} 989959.

Freitas, F.L. and Espíndola, J.J., 1993. "Noise and Vibration Reduction with Beam-Like Dynamic Neutralizers". *COBEM, 12th Brazilian Congress of Mechanical Engineering*.

Hudenski, R.A., Paraná, R.F. and Bavastri, C.A., 2007, "A Hybrid Electromechanical-viscoelastic Dynamic Vibration Neutralizer: A New Model and Analysis". *COBEM, 19th International Congress of Mechanical Engineering.*

Nagem, R.J., Madanshetty, S. and Medhi, G., 1995. "An Electromechanical Vibration Absorber". *Design Engineering Technical Conferences. ASME 1995.*Vol.3-part C, pp.53-57.

Paraná, R.F., 2008. "Neutralizador Dinâmico Híbrido Eletro-viscoelástico: Análise e Realização Experimental". Master Degree Dissertation, Universidade Tecnológica Federal do Paraná, Brasil.

Pritz,T., 1996. "Analysis of Four-Parameter Fractional Derivative Model of Real Solid Materials". *Journal of Sound and Vibration*, Vol.195 (1) 103-115.

Snowdon, J.C., 1968, "Vibration and Shock in Damped Mechanical Systems", John Wiley & Sons Inc., New York.

8. RESPONSIBILITY NOTICE